Nanocomposite Super-Swelling Hydrogels with Nanorod Bentonite

Z. Darvishi,[1] K. Kabiri,[2] M. J. Zohuriaan-Mehr,[2] A. Morsali[1]

[1]*Tarbiat Modares University, P.O. Box 14155-4838, Tehran, Iran*
[2]*Department of Color, Resin and Surface Coatings, Iran Polymer and Petrochemical Institute (IPPI), P.O. Box 14965-115, Tehran, Iran*

Received 16 January 2010; accepted 12 September 2010
DOI 10.1002/app.33417
Published online 14 February 2011 in Wiley Online Library (wileyonlinelibrary.com).

ABSTRACT: A modified bentonite (nanorod bentonite) was obtained from conventional bentonite by an ultrasonic treatment. Scanning electron microscopy (SEM) and transmission electron microscopy (TEM) images indicated that modified bentonite comprised rod-shape morphology without any change in the chemical structure confirmed by Fourier transform infrared (FTIR) spectroscopy and X-ray diffraction (XRD) patterns. Novel super-swelling hydrogels with nanocomposite structure were then prepared via solution polymerization of 2-acrylamido-2-methylpropane sulfonic acid (AMPS) and (*N*-[3-(dimethylamino)propyl] methacrylamide) (DMAPMA) in the presence of the nanobentonite and a crosslinker. The DMAPMA consisted of either intercalant or monomer in the polymerization. The hydrogel products were characterized by FTIR, swelling studies, dynamic mechanical thermal analysis (DMTA), XRD, and rheological measurements. It was proposed that exfoliated and intercalated morphology were obtained at low and high-nanobentonite contents, respectively. DMTA indicated that mechanical properties of the dried gel were improved with raising the clay content. In the water-swollen state, storage modulus was considerably increased in nanocomposites having <8% of modified bentonite, and then it was decreased at the higher clay content due to interfering effect of the clay in polymerization progression. J Appl Polym Sci 120: 3453–3459, 2011

Key words: hydrogel; swelling; nanocomposite; bentonite; ultrasonic modification

INTRODUCTION

Super-swelling hydrogels are polymers with ability to imbibe large amounts of water, saline solutions, or physiological fluids due to a considerable amount of hydrophilic groups in their structure.[1–4] The super-swelling characteristics of hydrogels make them ideal for use in water absorbing applications such as disposable diapers, cosmetics, absorbing pads,[1–4] agriculture,[5] coal dewatering,[6] sealing,[7] and controlled drug delivery systems.[8,9]

Hydrogels can be classified to cationic and anionic according to the nature of charges in polymer network. Because the structure and physical properties of ionic hydrogels can be altered by external stimuli (e.g., pH and temperature), they have been used for stimulus responsive drug-delivery systems.[10–12]

Highly swollen nanocomposites have been attracted a lot of efforts in the recent years.[13–15] The nanocomposites can be synthesized using modified clays, which have layered silicate structure.[14,15] Clays such as montmorillonite and bentonite have negative surface charges in their layers; they are mostly intercalated with using cationic materials such as alkyl ammonium salts.[16] Monomeric and polymeric materials such as chitosan[17,18] can also be used as intercalant. In comparison with conventional hydrogels, the nanocomposites have several advantages such as reducing cost and improving thermal,[14,19] mechanical,[15,19] or optical[18] properties.

In the present article, the novel hydrogels based on an anionic monomer 2-acrylamido-2-methylpropane sulfonic acid (AMPS) and cationic monomer *N*-[3-(dimethylamino)propyl] methacrylamide (DMAPMA) were prepared.

$$\mathbf{H_2C=CH-CONH-C(CH_3)_2-CH_2-SO_3H}$$
(AMPS)

$$\mathbf{H_2C=C(CH_3)-CONH-(CH_2)_3-N(CH_3)_2}$$
(DMAPMA)

Before the hydrogel synthesis, the modified bentonite (nanorod bentonite) was prepared through a sonication processing of bentonite.[20] The obtained hydrogel nanocomposites were characterized by X-ray diffraction (XRD), Fourier transform infrared (FTIR) spectroscopy, scanning electron microscopy (SEM), dynamic mechanical thermal analysis (DMTA), rheological, and swelling studies.

Correspondence to: M. J. Zohuriaan-Mehr (m.zohuriaan@ippi.ac.ir) or A. Morsali (morsali_a@yahoo.com).

TABLE I
Reactant Amounts and Conditions for the Polymerization Reaction to Prepare the Hydrogel Nanocomposites

	Nanobentonite content		Swelling capacity, g/g	
Sample code	Gram in synthesis	Weight percent	Distilled water	NaCl 0.9%
S0	0	0	62.5	–
S1	0.20	1.9	50.4	15.5
S2	0.40	3.7	44.4	10.4
S3	0.60	5.5	27.0	8.0
S4	0.80	7.2	29.0	7.6
S5	1.00	8.9	31.5	8.7
S6	0.60[a]	5.5	29.0	9.0
S7[b]	0.60	10.2	240.0	40.4
S8[c]	0.60	10.2	48.5	11.1

[a] Unmodified bentonite.
[b] Sample with no DMAPMA monomer.
[c] Sample with no AMPS monomer.

EXPERIMENTAL

Materials

Ammonium persulfate (APS) was supplied by Sinoharm Chemical Reagent Co. (Shanghai, China). AMPS, DMAPMA, poly(ethylene glycol) diacrylate (PEGDA, MW 330), and bentonite were supplied by Aldrich. Acetic acid was purchased from Merck. All the chemicals were used as received.

The bentonite modification

A suspension of bentonite and ethanol was sonicated with a certain power (90 W) by Sonicator-3000 (Misonix, Farmingdale, NY). Multiwave ultrasonic generator equipped with a converter/transducer and titanium oscillator (horn), 12.5 mm in diameter, and operating at 20 kHz with a maximum power output of 600 W, was used for the ultrasonic irradiation. The suspension was ultrasonically irradiated for 3 h with a high-density ultrasonic probe immersed directly into the solution. At the end of reaction, the suspension was filtered, and the filtrate was dried. Detailed procedure of the nanobentonite preparation reported elsewhere.[20]

The hydrogel preparation

Amounts of the starting materials used for all samples are given in Table I. AMPS (5.00 g, 0.024 mol) and DMAPMA (5.00 g, 0.029 mol) were dissolved in water (50 wt %) in a reactor. In the case of samples S7 and S8, no DMAPMA and AMPS was used, respectively. Acetic acid (3.0 mL), bentonite, and PEGDA (0.200 g in 2.0 g water) were then added to the reactor. It was stirred for 4 h to carry out possible intercalation reaction between cationic monomer and the clay. Consequently, initiator solution (0.050 g in 2.0 g water) was added to the reactor at room temperature. Then, the reactor was heated at $\sim$ 70°C to start polymerization reaction. Gelation was observed after 10–15 min. Following the gel point, the reactor was kept for 10 min the same temperature. The transparent elastic gel was removed from the reactor to cut into small pieces. The pieces were kept in air-forced oven at 70°C for 8 h.

Characterization

Swelling measurement

Dry sample powder (0.20 g) was immersed into distilled water (70 mL) or 0.9% sodium chloride solution (50 mL) for $\sim$30 min to reach the equilibrium swelling. Then, it was filtered and weighed. Swelling capacity (Q) was determined by eq. (1).

$$Q = [(m - m_0)/m_0] \quad (1)$$

where m is the mass of swollen gel and m_0 the mass of initial dried sample.

X-ray diffraction

The X-ray powder diffraction (XRD) measurements were performed using a Philips diffractometer of X'pert Company with mono chromatized Cu Kα radiation. The crystallite sizes of selected samples were estimated using the Sherrer method.

Infrared spectra

IR spectra were recorded on a Shimadzu-IR460 spectrometer in a KBr matrix.

Rheology

The rheological measurements were performed on the samples each absorbed a fixed amount of water (0.30 sample in 5.0 g water). A Paar–Physica

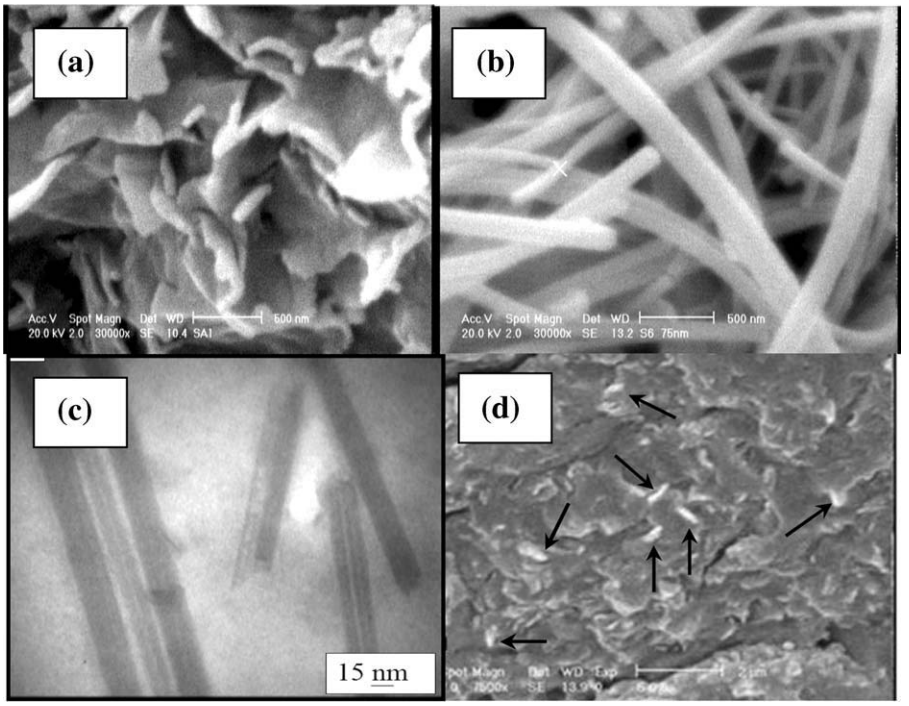

Figure 1 (a) SEM micrograph of unmodified bentonite. Pictures (b) and (c) are SEM and TEM of the modified bentonite, respectively. (d) SEM picture of the nanocomposite hydrogel with 5.5% modified bentonite.

oscillatory rheometer (MCR300, Germany) at 25°C with parallel plate geometry (plate diameter of 25 mm, gap of 3 mm) was used for the analysis. The detailed procedure was previously reported.[21]

Scanning electron microscope

The samples were characterized with a scanning electron microscope (SEM; Philips, The Netherlands, Model XL30) with gold coating.

Transmission electron microscope

A transmission electron microscope (TEM, Zeiss CEM 902 A) was used for the morphological studies. The bentonite sample was dispersed very well in water before using for the analysis.

Dynamic mechanical thermal analysis

Dynamic mechanical thermal analysis (DMTA) of the powdery sample was performed using a Polymer Laboratories Instrument. The experiments were carried out in the temperature range 80–160°C, heating rate 20°C/min, and frequency 1 Hz.

RESULTS AND DISCUSSION

Bentonite modification

A sonochemical modification method was used to simply prepare the rod-shaped bentonite from the conventional bentonite.[20] Figure 1 shows SEM and TEM image of modified bentonite before and after sonication treatment, respectively. As it is obvious from Figure 1(b), it had rod-shape morphology after treatment. These images show that modification process is successfully carried out to convert bentonite from particulate shape to the rodlike shape. The nanometric dimensions of the bentonite rods are obviously exhibited in Figure 1(c).

Particle-size distribution of the modified bentonite was also measured (Fig. 2). The rod diameters were found to be between 5 and 55 nm; however, the majority (more than 80%) of rod diameters was between 35 and 55 nm.

Figure 1(d) shows SEM micrograph of hydrogel noncomposite contained 5.5% nanobentonite. Few rod-shaped nanobentonite particles can be observed (shown by arrows on the picture). It can be concluded that of nanorod bentonite particles have been properly dispersed in the polymer matrix, and agglomeration has not been occurred.

Hydrogel synthesis and spectral characterization

Poly(AMPS-DMAPMA) gels were synthesized via solution polymerization using a persulfate initiator (APS) in the presence of a macrocrosslinker, PEGDA, under normal conditions. Because DMAPMA exists in its cationic form in the acidic medium, we used this comonomer mainly due to achieve the intercalation of bentonite. Thus, before the addition of the

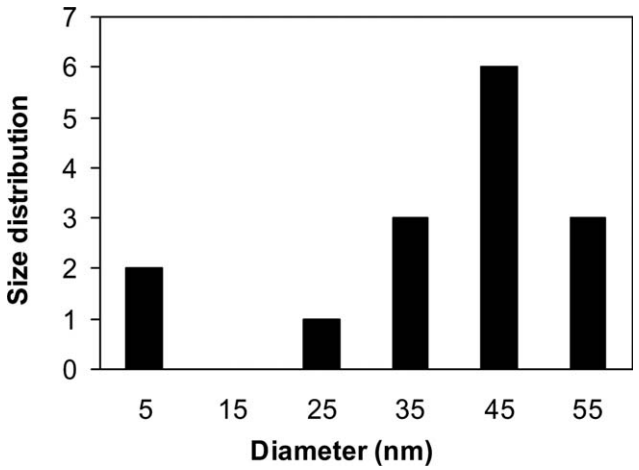

Figure 2 Particle size histogram of the modified bentonite (nanorod bentonite).

initiator, the dispersion was mixed for 4 h to attain intercalation of DMAPMA monomer into the clay galleries. Table I gives the sample encoding and weight percentages of the clay in each sample. Representatively, gel content (as a measure of the yield of gel synthesis) of two counterpart samples S3 and S6 was determined to be 63 and 50 wt %, respectively. It succinctly showed the constructive effect of the modified bentonite on the crosslinking polymerization. Higher gel content of S3 preliminarily verified that the modified clay (nanorod bentonite) particles have been involved in the gel network formation much more efficient than the unmodified one. This action will be reconfirmed in the sections swelling and rheological studies.

IR spectra of the nanorod bentonite and the initial bentonite material were nearly identical. The relatively weak absorption bands around 3600–3300 cm^{-1} are ascribed to O—H stretching vibration. The sharp absorption peaks at 1035 cm^{-1} corresponds to the stretching vibration of Si—O bond. The peaks at 471–526 cm^{-1} are due to bending of Si—O vibration, and the peak at 800 cm^{-1} may be attributed to the stretching vibration of Al—O—Si.[22] The bands at 3396 and 1653 cm^{-1} are due to adsorbed water molecules. The band at 1031 cm^{-1} has been attributed to the asymmetric stretching modes of Si—O—Si. The OH-bending bands are appeared at 985 cm^{-1}.[23–25]

In the spectra of poly(AMPS-DMAPMA) gel samples, a very broad band around 3330 cm^{-1} was observed due to the OH of the moisture absorbed by the hydrogel. This strong broad band overlaps the secondary amide N—H stretching band. The sharp strong to medium bond due to unsymmetrical and symmetrical stretching C—H are appeared at ~2995 and ~2845 cm^{-1}. Stretching vibration bands of C—S and the amide C=O are appeared at 610 and 1640 cm^{-1} as sharp peaks, respectively. The CH_2 and CH_3 bending bands are appeared at 1465 and 1390 cm^{-1}, respectively. Finally, a weak peak due to the secondary amide N—H bending is appeared at 1554 cm^{-1}. Symmetrical and unsymmetrical stretching vibration bands of O=S=O are appeared at 1174 and 1397 cm^{-1} as sharp peaks, respectively.

Swelling studies

The data of Table I shows swelling capacity dependence on the clay content of the hydrogel nanocomposite in distilled water and saline solution. Swelling capacity was decreased with clay content enhancement. The swelling of the clay-free sample in water (62 g/g) was reduced to 31 g/g for the sample with clay content 8.9%. All the swelling values were expectedly decreased in saline solution. It is related to decrease of osmotic pressure difference between the gel phase and swelling media.[1,2] Water-swelling reduction in lieu of more clay content can be attributed to crosslink role of the nanorod bentonite particles. They can act as crosslink points or multifunctional crosslinkers, which increased crosslink density.[14,15] Haraguchi mentioned that hydrogel nanocomposite may be formed even without crosslinker. Clay particles can be exfoliated in polymeric matrix; and interaction between exfoliated clay and polymeric chains creates crosslinks. Multifunctionality of clay was calculated to be around 50 for poly(*N*-isopropyl acrylamide)-laponite hydrogel nanocomposites.[26] Therefore, the swelling loss might be originated from the increase of clay content resulted in enhanced crosslink density.

It was found that when the nanobentonite was used instead of the unmodified clay, the swelling was decreased. For example, swelling of S6 (29 g/g in water and 9 g/g in saline) was decreased (27 g/g in water and 8 g/g in saline) by using the nanobentonite (sample S3, Table I). This observation verifies that the nanobentonite action as the multifunctional crosslinker is more than that of the unmodified bentonite.

Finally, it should be pointed out that sample S7 with no cationic monomer (DMAPMA) exhibits a superabsorbency behavior (240 g/g in water and 40 g/g in saline). The reason comes back to the high percentage of the clay (as a polymerization interferer factor). In addition, nearly non of this high clay content (10.2 wt %) can be intercalated by the anionic monomer AMPS. More importantly, AMPS is a strong organic acid, and so it is totally dissociated in water favoring the highly improvement of the swelling capacity. Actually, in the copolymeric samples S0–S6, the protonated DMAPMA obstructs the repulsion forces (as the one of the main factors of swelling in water). That is why the overall swelling

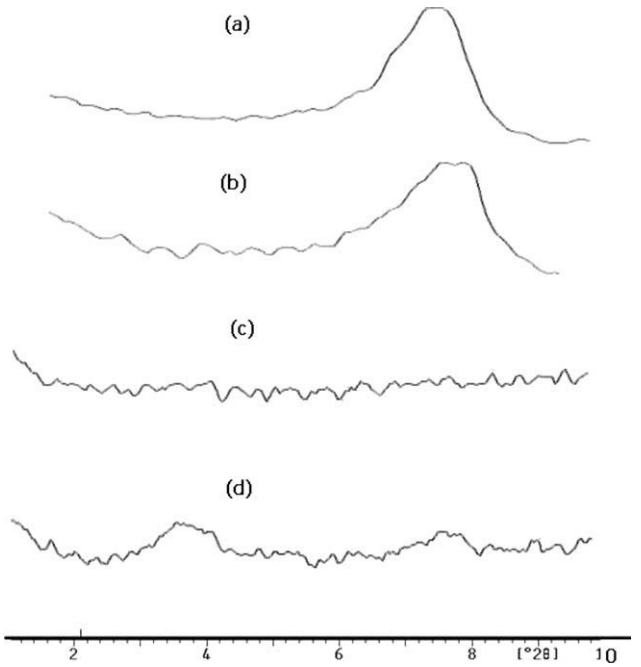

Figure 3 The XRD patterns of (a) bentonite, (b) modified bentonite, (c) and (d) are the patterns for samples S1 and S4, respectively.

capacity of the copolymeric samples is not as high as that of sample S7.

XRD study

Figure 3 shows X-ray diffraction (XRD) patterns of unmodified and modified bentonite as well as the hydrogel nanocomposites with different amounts of modified bentonite. Because the Figure 3(a,b) is identical, they indicate that the bentonite modification process (the sonochemical treatment) has no effect on the fundamental character of the clay crystalline structure. No diffraction peak for nanocomposite hydrogels having 1.9% bentonite is observed [Fig. 3(c)]. This can be attributed to exfoliated structure in nanocomposite hydrogels. In this state, crystalline structure was destructed, and no peak was observed in diffraction pattern. Because of the cationic nature of DMAPMA, this cation can be exchanged with the sodium cations of clay layers during the premixing at room temperature. These intercalated monomers (as well as the nonintercalated ones) are then polymerized to obtain the exfoliated structure in the polymer matrix.

In the sample with higher clay (7.2% clay; sample S4), however, two diffraction peaks were observed at 2θ 7.49°–7.73° and 3.65°–3.89° [Fig. 3(d)]. These peaks were related to nonintercalated and intercalated bentonites, respectively. Because the cationic monomer content was fixed in all the samples, it could not be exchanged between all the clay layers. As a result, the peak of 2θ 7.73° can be related to nonintercalated clay particles. A shifted peak at 2θ 3.65°–3.89° indicates the intercalated layers formed via the monomer exchanging with the clay cations. The high-clay content (7.2%) prevents to reach an exfoliated structure. Similar behavior was previously reported for poly(AMPS).[17]

Rheological study

Figure 4(a) shows rheological behavior for the water swollen samples of clay-free hydrogel (sample S0) and those of containing different amounts of the modified bentonite. Storage modulus has an ascending trend with increase of modified bentonite up to 7.2 wt %. For instance, storage modulus was

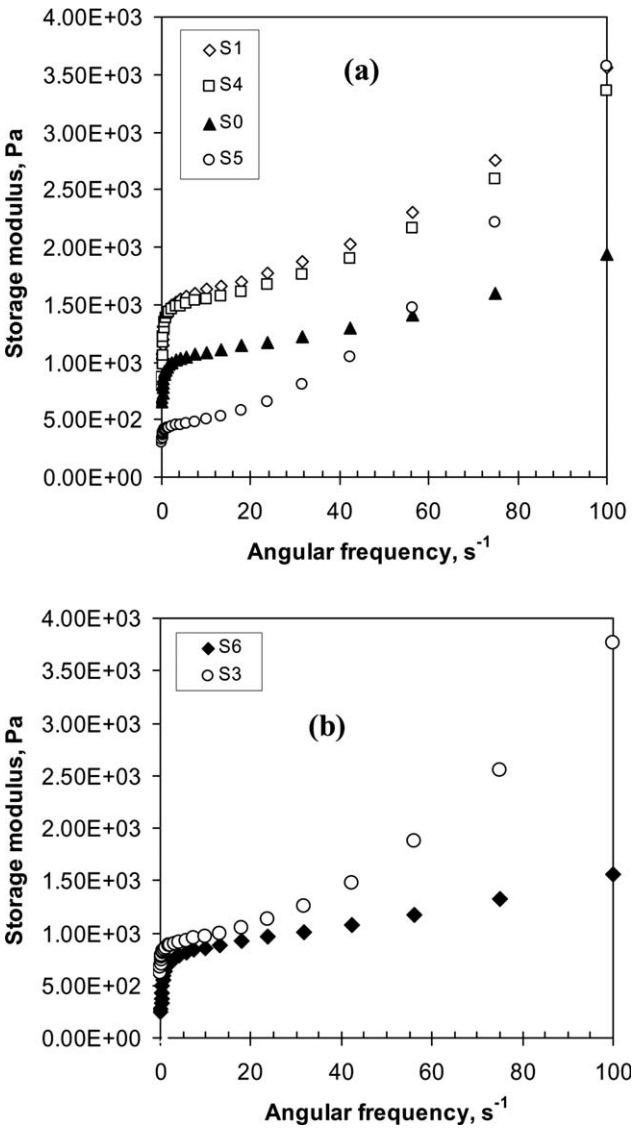

Figure 4 Rheological behavior of hydrated gels for (a) samples containing different amounts of modified bentonite and (b) samples with fixed amounts of modified (S3) and unmodified (S6) bentonite.

1220 Pa for S0 measured at angular frequency 31.9 s^{-1}. It was increased as high as 44 and 53 percentages in the samples containing 7.2 wt % and 1.9 wt % modified bentonite, respectively. The modulus was then decreased with increasing the modified bentonite up to 8.9 wt % (sample S5). The reason for increase of storage modulus with increase of clay content can be attributed to crosslinking role of the clay. Storage modulus has relationship with average molecular weight between crosslinks (M_c) eq. (2).

$$G' = \rho RT/M_c \quad (2)$$

where G' is the relaxed rubbery modulus, ρ is density, R is the gas constant, and T is temperature. The M_c has inverse relationship with G', so that it is decreased with increase of the clay content at low-clay percentage led to increased storage modulus. At high-clay content (sample S5 with 8.9 wt % modified bentonite), two parameters are simultaneously involved in crosslink formation. First, the clay can play a crosslinking role due to its multifunctionality characteristics. Second, viscosity enhancement of the solution polymerization at high-clay content disfavors polymerization progress. In a viscose media, probability addition of monomer and particularly crosslinker to the polymer network is reduced. Therefore, it is possibly some part of the chemical crosslinker does not involve in the crosslinking polymerization. As a result, M_c is increased, and storage modulus is reduced. Similar rheological behavior has been observed for poly(AMPS) nanocomposites.[15]

As shown in Figure 4(b), the copolymer S3 (with 5.5 wt % modified bentonite) exhibited higher modulus rather than the counterpart hydrogel having the same amount of unmodified bentonite, S6. Similar to foresaid explanation on the swelling capacity studies, this discrimination may be attributed to the multifunctional crosslinking role of the modified bentonite nanoparticles, which is more efficient than the unmodified bentonite particles.

Dynamic mechanical thermal analysis study

Thermomechanical properties of the hydrogels were studied by dynamic mechanical thermal analysis (DMTA). Tan δ versus temperature is shown in Figure 5(a) for dried poly(AMPS-DMAPMA) samples with different clay contents. Tan δ is considerably reduced with clay content enhancement. This indicates that higher clay content reduces dissipation ability of the polymer chains. Clay has no viscoelastic properties and movement due to applied stress like polymers. Therefore, increase of clay content decreases viscose properties of the network led to decrease of tan δ.

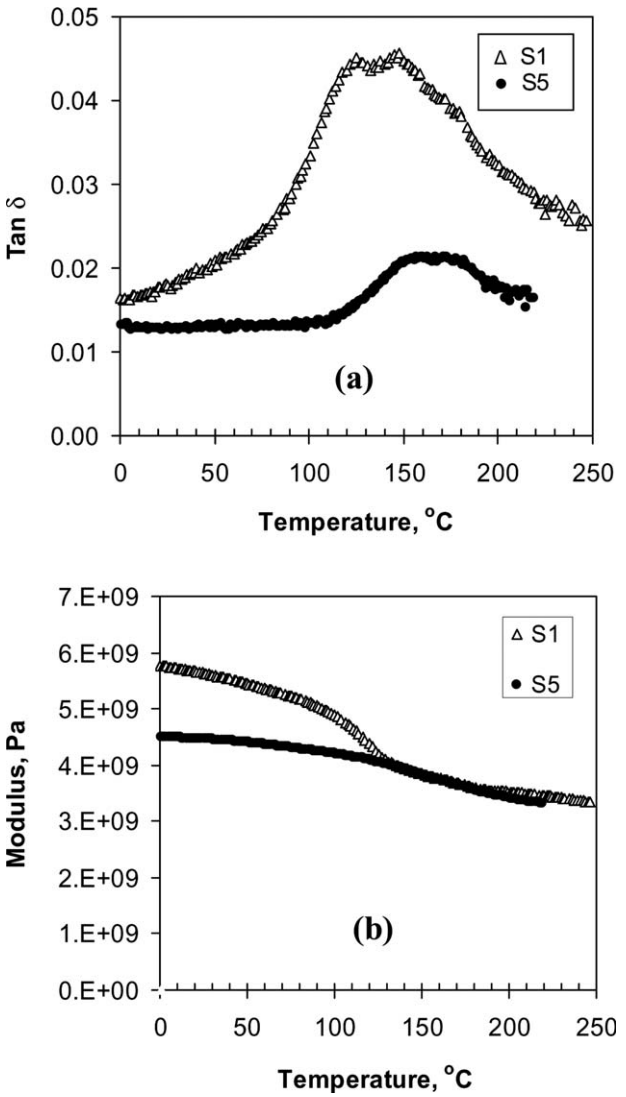

Figure 5 DMTA analysis of dried samples S1 and S5. (a) Tan δ and (b) storage modulus versus temperature.

The tan δ peak, indicating the glass transition temperature, has expectedly been shifted to higher temperatures when the sample is included higher bentonite incorporated [Fig. 5(a)]. Two T_g values are observed in the figure. The greater one may preliminarily be attributed to the possible zones of aggregated nanoparticles.

Figure 5(b) shows storage modulus of poly(AMPS-DMAPMA) versus temperature for the samples having 1.9 and 8.9% modified bentonite (i.e., samples S1 and S5). Rheological studies give modulus in the swollen state, while DMTA shows modulus of the dried gel. Below T_g, modulus of sample S1 is significantly higher than that of sample S5, but the rubbery modulus of both samples is quite identical. This discrimination, indicated the crosslinking role of clay,[14–17] is more pronounced in low-clay content. These additional bentonite-based crosslinks, which increase modulus below T_g, probably are de-

crosslinked with increase of temperature. As a result, similar rubbery modulus is observed for both samples. On the other hand, the modulus loss may also be related to the reinforcement effect of clay. Around T_g and higher, the material becomes soft, and the clay strengthening effect is prominent due to the restricted movement of the polymer chains surrounding the clay platelets.[27] Therefore, the thermally induced loss of modulus for the sample S5 will be less than that of S1. The overall reinforcement of the nanocomposite benefits from the potential bonds between the polymer and the bentonite layers. The modulus of the composite is expected to be influenced by the modulus of the matrix, the modulus of the clay, and the shape and orientation of the clay particles.[28]

The higher modulus below T_g for comparing to S5 containing can also be related to the morphology difference. As previously shown in section XRD studies, the samples S1 with 1.9% modified bentonite possess exfoliated structure, while S5 having 10% of the clay have to be intercalated. The morphology-dependency properties such as modulus and T_g of polymer nanocomposite have already been studied.[29]

CONCLUSIONS

Modified bentonite (nanobentonite) was achieved through a sonication process. SEM and TEM images confirmed that the modified clay had nanorod shape morphology. It was found that the amine-containing monomer DMAPMA had two roles in synthesis of poly(AMPS-DMAPMA)/nanobentonite gel product; intercalant and comonomer. Cationic nature of DMAPMA led to copolymer nanocomposite with exfoliated structures by incorporating low content of the nanobentonite (i.e., <4 wt %). It was also found that the modified bentonite had constructive effect on the gel network formation in comparison with that of the unmodified bentonite.

Rheological studies on the water-swollen samples showed that storage modulus was increased in comparison with the clay-free counterpart. This loss of stiffness at high-clay content was attributed to inhibiting role of clay in the polymerization, particularly due to high viscosity of polymerization mixture.

DMTA analysis on dried samples showed that dissipation ability is considerably decreased with increase of the clay content. Modulus below T_g was considerably higher at low-clay content. It was ascribed to the morphology difference, that is, exfoliated versus intercalated structure.

References

1. Buchholz, F. L.; Graham, T. Modern Superabsorbent Polymer Technology; Wiley-VCH: New York, 1998.
2. Zohuriaan-Mehr, M. J.; Kabiri, K. Iran Polym J 2008, 17, 451.
3. Riccardo, Po. J Macromol Sci-Rev Macromol Chem Phys 1994, 34, 607.
4. Available from <http://www.eng.buffalo.edu/Courses/435/Diares/Diapers.html>.
5. Mohan, Y. M.; Geckeler, K. E. React Funct Polym 2007, 67, 144.
6. Dzionmwa, G. P. T.; Wood, C. J.; Hill, D. J. T. Polym Adv Technol 1997, 8, 767.
7. Sun, X.; Zhang, G.; Shi, G.; Tang, B.; Wu, Z. J Appl Polym Sci 2002, 86, 3712.
8. Dorkoosh, F. A.; Brusee, J.; Verhoef, J. C.; Borchard, G.; Tehrani, M. R. Polymer 2000, 41, 8213.
9. Chen, J.; Park, K.; Park, H. J Control Rel 2000, 65, 73.
10. Heller, J. In Controlled Drug Delivery: Challenges and Strategies; Park, K., Ed.; ACS, Washington, DC, 1997; p 127.
11. Wu, X. Y.; Arshady, Q. R. In Polymeric Biomaterials; Arshady, R., Ed.; Citus Books: London, UK, 2003; p 157.
12. Wu, X. Y.; Arshady, Q. R. In Polymeric Biomaterials; Arshady, R., Ed.; Citus Books: London, UK, 2003; p 195.
13. Lin, J. M.; Wu, J. H.; Yang, Z. F.; Pu, M. L. Macromol Rapid Commun 2001, 22, 422.
14. Haraguchi, K.; Takenisa, T.; Fan, S. Macromolecules 2002, 35, 10162.
15. Kabiri, K.; Mirzadeh, H.; Zohuriaan-Mehr, M. J.; Daliri, M. Polym Int 2009, 58, 1252.
16. Kabiri, K.; Mirzadeh, H.; Zohuriaan-Mehr, M. J Iran Polym J 2007, 16, 147.
17. Kabiri, K.; Mirzadeh, H.; Zohuriaan-Mehr, M. J. J Appl Polym Sci 2010, 116, 2548.
18. Ravi, N.; Aliyar, H. A.; Hamilton, P. D. Macromol Symp 2005, 227, 191.
19. Li, A.; Wang, A.; Chen, J. J Appl Polym Sci 2004, 92, 1596.
20. Darvishi, Z.; Morsali, A. Ultrasonics Sonochem 2010, 18, 238.
21. Ramazani-Harandi, M. J.; Zohuriaan-Mehr, M. J.; Yousefi, A. A.; Ershad-Langroudi, A.; Kabiri, K. Polym Test 2006, 25, 470.
22. Frost, R. L.; Cash, G. A.; Kloprogge, J. T. Vibrat Spectrosc 1998, 16, 173.
23. Frost, R. L.; Locos, O. B.; Ruan, H.; Kloprogge, J. T. Vibrat Spectr 2001, 27, 1.
24. Madejova, J. Vibrat Spectr 2003, 31, 1.
25. Melo, D. M. A.; Ruiz, J. A. C.; Melo, M. A. F.; Schmall, M. Microporous Mesoporous Mater 2000, 8, 345.
26. Nie, J.; Du, B.; Oppermann, W. Macromolecules 2005, 38, 5729.
27. Diaconu, G.; Paulis, M.; Leiza J. R. Polymer 2008, 49, 2444.
28. Nobel, M. L.; Mendes, E.; Picken, S. J. J Appl Polym Sci 2007, 104, 2156.
29. Meneghetti, P.; Qutubuddin, S. Thermochim Acta 2006, 442, 74.